



Pergamon

Available online at www.sciencedirect.com

SCIENCE @ DIRECT®



www.actamat-journals.com

Acta Materialia 51 (2003) 1351–1357

Mechanics of thin ultra-light stainless steel sandwich sheet material

Part II. Resistance to delamination

A.E. Markaki, T.W. Clyne *

Department of Materials Science and Metallurgy, University of Cambridge, Pembroke Street, Cambridge CB2 3QZ, UK

Received 2 April 2002; accepted 30 October 2002

Abstract

This study concerns three variants of a novel type of thin sandwich sheet. Details of the core structures, and also the results of an investigation into elastic properties, were presented in the first part of this pair of papers. A study was also made of the tensile properties of single fibres of the type present in the core of these sheets. In this second paper, an investigation is presented of the resistance offered by these materials to delamination of the two faceplates. In one variant of the material, in which the fibres lie approximately normal to the plane of the sheet, delamination occurs predominantly by frictional pull-out of fibres from their sockets in the adhesive. The mode I fracture energy has been measured at about 340 J m^{-2} . This value is consistent with predictions from a model based on shear-lag theory, with a fibre–adhesive interfacial shear strength of about 5 MPa. It is noted that there should be scope for improving the fracture energy somewhat by raising the strength of the fibre–adhesive bond. For the other two variants studied, in which the fibres are softer (as a result of heat treatment during sintering) and are inclined close to the plane of the sheet, the measured fracture energy is appreciably lower at about 30 J m^{-2} . In this case, delamination occurs by fracture of the fibres near the mid-plane. Application of a simple model for prediction of the fracture energy in this case leads to the conclusion that some of the fracture was probably of sintered necks between fibres, rather than the fibres themselves, and that this process required considerably less energy.

© 2003 Acta Materialia Inc. Published by Elsevier Science Ltd. All rights reserved.

Keywords: Stainless steel; Lightweight materials; Sandwich panels; Steel fibres; Composite materials; Fibre pull-out; Interfacial fracture energy

1. Introduction

As was outlined in Part I, there has been extensive interest recently in the development of light-

weight metallic sheets with a porous core. The current work relates to a thin ($\sim 1 \text{ mm}$) sandwich sheet with $200 \mu\text{m}$ thick faceplates and a core containing metallic fibres. In Part I, structural details were presented of three variants of such a material and their stiffness characteristics were examined. This second paper explores the resistance that they offer to delamination (separation of the faceplates). Such

* Corresponding author. Fax: +44-01223-334567.

E-mail address: twc10@cam.ac.uk (T.W. Clyne).

information is needed if the core structures are to be optimised in a systematic way, although it is, of course, important to note that factors affecting other properties, such as formability, weldability, damping behaviour, ease of production etc. are also likely to be relevant.

2. Experimental procedures

2.1. Materials

Details of the production and microstructural characteristics of the three variants (HSSA, CAMBOSS and CAMBRASS) were given in the first paper. Basically, the fibres lie approximately normal to the plane of the sheet in the HSSA material, and are adhesively bonded to the faceplates. The other two materials are made by bonding a sintered fibre mesh to the faceplates, either by adhesive bonding (CAMBOSS) or by brazing (CAMBRASS).

2.2. Interface fracture energy measurements

The resistance of these duplex sheets to becoming torn apart is an important property, since this will influence the deformation and fracture behaviour both during forming and under service conditions. This resistance is best characterised in terms of the energy absorbed when the faceplates are separated. The work of fracture for debonding of the faceplates from the core has been measured for mode I loading conditions. It may be noted that, due to the low (in plane) shear stiffness of the core in these materials (see Part I), the mode I interfacial fracture energy is not expected to be very different from that measured under mixed mode loading conditions.

The test fixture employed [1] allows in situ observation in a scanning electron microscope of crack propagation. A specimen was adhesively bonded between two steel plates whose ends were loaded with pure bending moments M , as shown in Fig. 1. Prior to testing, a narrow pre-crack was introduced into the beam mid-plane. The strain energy release rate under steady-state conditions is given by [1]

$$G = 12(1-\nu^2) \frac{M^2}{Eb^2H^3} \quad (1)$$

where E and ν are Young's modulus and Poisson's ratio, b the width and H is the half-thickness of the test specimen.

3. Results

3.1. HSSA sheets

It was observed that HSSA sheets underwent delamination predominantly by the fibres being pulled out of their sockets in the adhesive layer. This is illustrated in Fig. 2. The average measured value of the (mode I) fracture energy was found to be about 340 J m^{-2} . This is quite a substantial value for an interfacial fracture energy and indicates that delamination will not occur very readily during handling and processing (and, if it does take place, for example under crash conditions, then the associated energy absorption may well be significant).

3.2. CAMBOSS and CAMBRASS sheets

CAMBOSS and CAMBRASS sheets were observed to delaminate within the core itself, rather than at the interfaces with the faceplates. This is illustrated in Fig. 3. It can be seen that some fibre fracture has occurred, and also that some sintered necks between fibres have failed. The fracture energies were found to be appreciably lower than for the HSSA material. The average measured value of the (mode I) fracture energy was about 30 J m^{-2} . There were no systematic differences between the behaviour of the two types of sheets, which is unsurprising since they differ only in the way that the fibres are attached to the faceplates and in all cases the fracture and deformation was confined to the mid-plane region.

4. Modelling of energy absorption during interfacial delamination

4.1. Fibre pull-out in HSSA sheets

A simple model has been developed for delamination in the HSSA material, based on a shear-lag

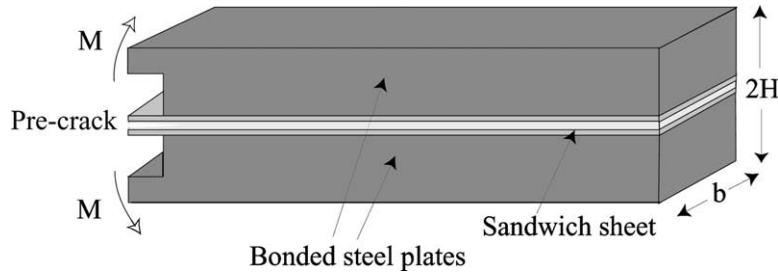


Fig. 1. Schematic of the specimen geometry used for measuring mode I interface fracture resistance.

treatment of fibre pull-out [2]. Consider an inclined fibre with a diameter d and an embedded length x , as illustrated in Fig. 4. The work done in pulling out a single inclined fibre can be written as

$$\Delta G = \int_0^{L/\sin\theta} \pi dx \tau_{i*} = \pi d \frac{L^2}{2\sin^2\theta} \tau_{i*} \quad (2)$$

where τ_{i*} is the fibre–adhesive interfacial shear strength, taken as constant along the fibre length. If the number of fibres per unit area is written as N , there will be $(N\sin\theta dx/L)$ per unit area with an embedded length between x and $(x + dx)$. Thus the total work done in pulling out the inclined fibres, G_{fp} is given by

$$G_{fp} = \int_0^{L/\sin\theta} \frac{N\sin\theta dx}{L} \pi d \frac{L^2}{2\sin^2\theta} \tau_{i*} \quad (3)$$

As was outlined in Part I, the number of fibres per unit area, N , is related to the fibre volume fraction, f , and the fibre diameter, d by

$$N = \frac{4f\sin\theta}{\pi d^2} \quad (4)$$

Substituting this expression into Eq. (3) and integrating (assuming equal embedded lengths for all fibres) leads to

$$G_{fp} = \frac{2f\tau_{i*}L^2}{d\sin\theta} \quad (5)$$

Fig. 5 shows the predicted dependence of this pull-out energy on interfacial shear strength. From SEM images, such as that shown in Fig. 6, it can be estimated that the fibres are typically anchored

into the adhesive to a depth of about $100 \mu\text{m}$ ($=L$). It can be seen that the experimentally obtained value of G ($\sim 340 \text{ J m}^{-2}$) corresponds to that predicted by the model (using $f = 0.08$, $L = 100 \mu\text{m}$, $\theta = 75^\circ$ and $d = 25 \mu\text{m}$) if the fibre–adhesive interfacial shear strength has a value of about 5 MPa . This is a relatively low value for an interfacial shear strength [3,4], although it is certainly of the order of magnitude expected.

Note that it should be possible, by raising the strength of the fibre–adhesive bond and controlling the embedded fibre lengths and orientations, to inhibit pull-out and promote other energy-absorbing mechanisms, such as plastic deformation and rupture of the fibres, which in principle have the potential for greater energy absorption. An estimate of the contribution from fibre fracture, G_{fr} can be made by the expression

$$G_{fr} = NU_d h_f \quad (6)$$

where N , from Eq. (4), is about $1.5 \times 10^8 \text{ fibres m}^{-2}$, U_d the work of fracture for a single as-drawn fibre (0.005 J m^{-1} —see Part I) and h_f is the fibre length ($\sim 0.8 \text{ mm}$ —see Part I). This assumes that complete fibre lengths undergo deformation of the same type as they exhibit during single fibre tensile testing. It leads to an estimated value for G_{fr} of about 640 J m^{-2} . This calculation assumes that all the fibres in the core rupture, so that this value represents the upper bound. Nevertheless, the contribution from this mechanism is potentially larger than that from fibre pull-out. The interfacial shear strength needed for the fibres to break can be estimated using a shear-lag balance

$$\tau_{i*} = \left(\frac{d}{4h_f} \right) \sigma_{f*} \quad (7)$$

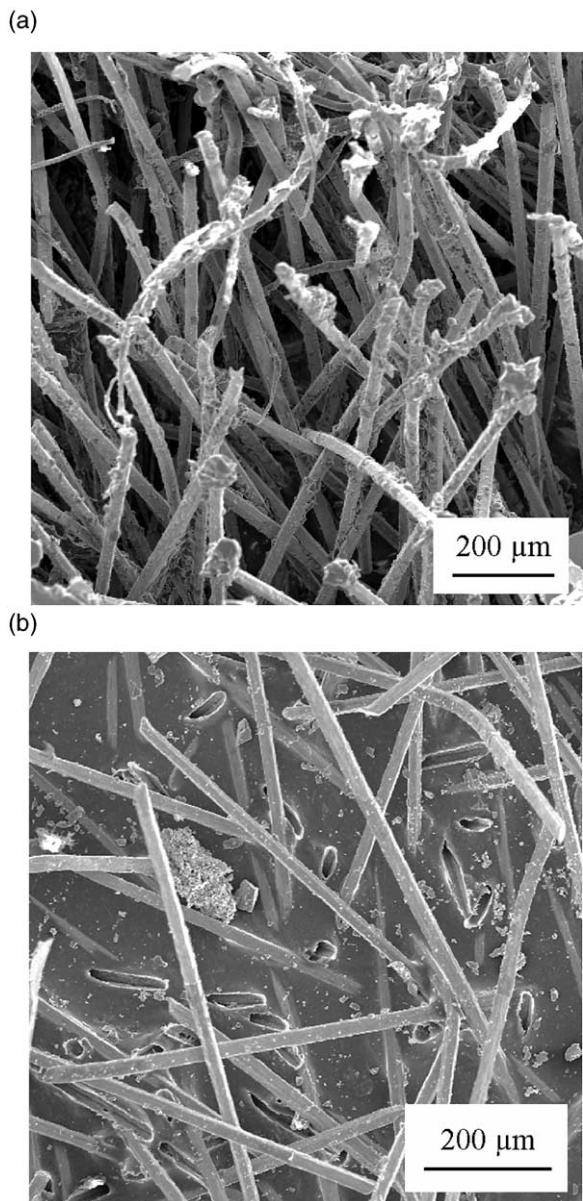


Fig. 2. Scanning electron micrographs of the fracture surface from an HSSA sheet showing: (a) glue attached on the ends of the inclined fibres, and (b) the sockets of the adhesive layer from which the fibres were pulled out.

where σ_{f*} is the stress required for the as-drawn fibres to break, which was measured as about 1.2 GPa (see Part I). The shear stress is thus about 10 MPa, which is higher than the shear stress required for fibre pull-out (~ 5 MPa). Since the fibre–

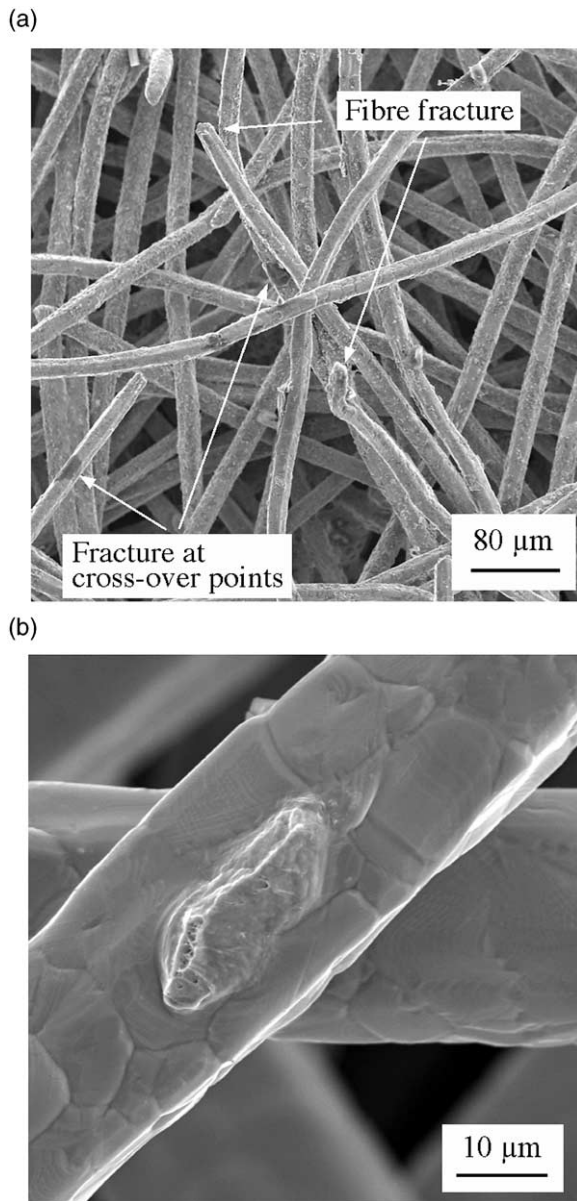


Fig. 3. Scanning electron micrographs showing: (a) (plan view) of the fracture surface from a CAMBRASS sheet, and (b) neck formed at fibre crossings from a CAMBOSS sheet.

adhesive interface cannot sustain such a stress, the fibres pull out instead of fracturing. An increase in the fibre–adhesive shear strength would, therefore, lead to an increase in the fracture energy.

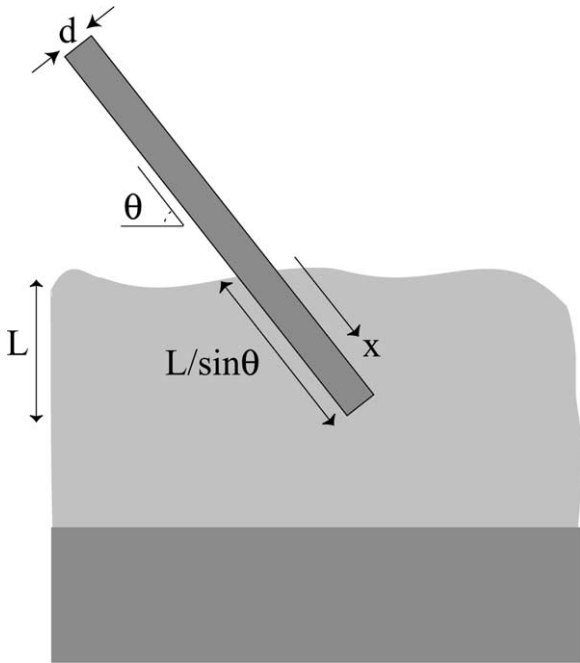


Fig. 4. Schematic of the model used for prediction of energy absorption during pull-out of inclined fibres for the HSSA core.

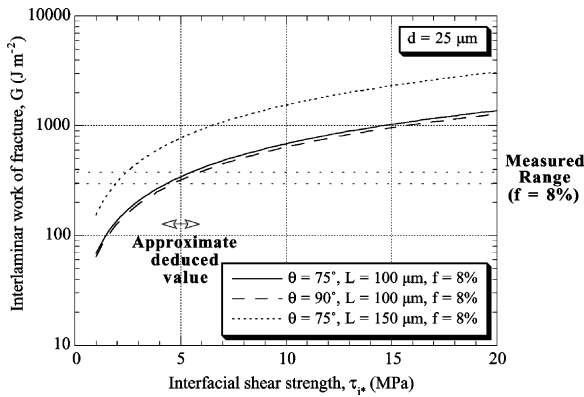


Fig. 5. Predicted dependence of the interlaminar fracture energy of the HSSA core on the fibre–adhesive interfacial shear strength.

4.2. Fibre fracture in CAMBOSS and CAMBRASS sheets

CAMBOSS and CAMBRASS sheets are observed to delaminate by fibre fracture. A simple model has been developed to estimate the fracture energy for this mechanism. It is assumed that all

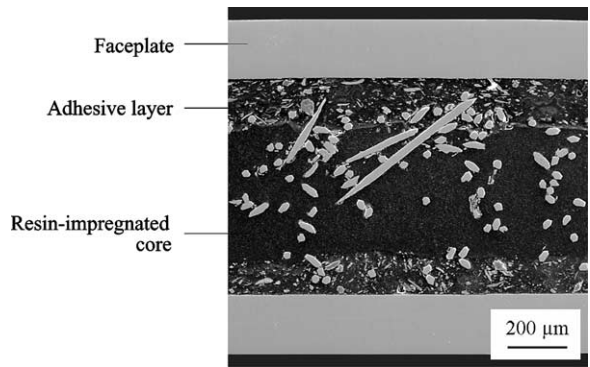


Fig. 6. Scanning electron micrograph showing a section through the HSSA sheet, after impregnation of the cavity in the core with resin and subsequent polishing.

the fibres deform and fracture within a deformation zone of length z . This is illustrated in Fig. 7. The work of fracture may then be written as

$$G_{fr} = NU_s z \tag{8}$$

where U_s is the work of fracture for a single sintered fiber ($\sim 0.0011 \text{ J m}^{-1}$ —see Part I). Substituting the expression for N given in Eq. (4) into Eq. (8) leads to

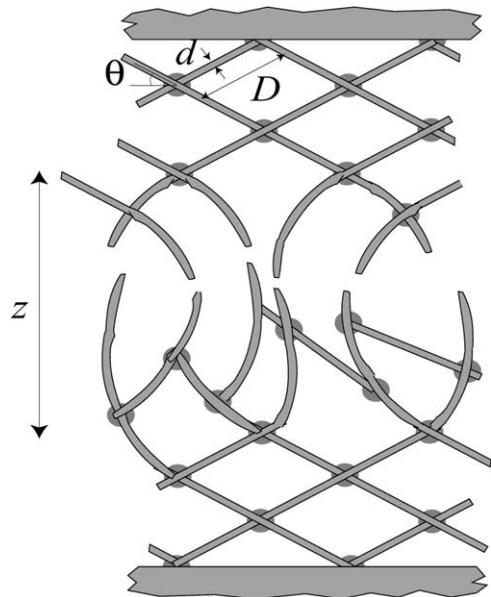


Fig. 7. Schematic of the model used for prediction of energy absorption during fibre fracture for the CAMBOSS and CAMBRASS cores.

$$G_{fr} = \left[\frac{4f \sin \theta}{\pi d^2} \right] U_{ss} \quad (9)$$

Predictions obtained using this equation are shown in Fig. 8. The experimental value G ($\sim 30 \text{ J m}^{-2}$) is consistent with model predictions if the fibres are inclined at 5° to the plane of the sheet and the deformation zone is about $100 \mu\text{m}$ long. Evidently, the length of the deformation zone is an important parameter and these results suggest that deformation is restricted to a fairly narrow band. This is not something that can readily be verified by inspection of failed specimens, since it is rather difficult to establish precisely where substantial plastic deformation of the fibres has occurred. Nevertheless, the general impression on inspecting the damage and deformation zone is that it was wider than $100 \mu\text{m}$. However, it can be seen from Fig. 3 that some failure occurred at the sintered necks, rather than by fibre fracture. As illustrated in Fig. 3(b), the width of the necks can be quite small, relative to the fibre diameter. Consequently, when the faceplates are torn apart, necks that are not sufficiently strong are apparently quite prone to fail. This might account for the measured fracture energy being low and for it being necessary to postulate low values of θ and z in order to get good agreement between model and experiment.

An important issue in this context is the concept of generating a fibre microstructure that gives the

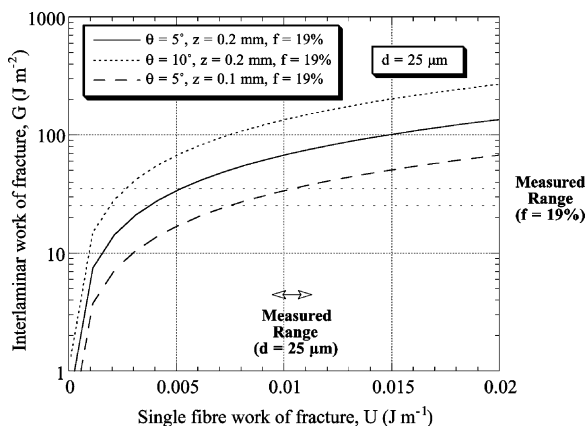


Fig. 8. Predicted dependence of the interlaminar fracture energy of the CAMBOSS and CAMBRASS core on the single fibre work of fracture.

desired combination of strength and toughness. There is considerable scope for achieving this with austenitic stainless steel fibres, which can be cold worked (e.g. drawn) to induce martensite formation and then subjected to various heat treatments (tempering) to control grain structure and carbide formation. In general, it should be possible to tailor core geometries and fibre properties so as to generate relatively high fracture energies for both fibre pull-out and fibre fracture failure modes.

5. Conclusions

The following conclusions can be drawn from this work.

- (a) The fracture energy during delamination has been measured for three variants of a novel type of thin sandwich sheet, under pure mode I loading. For the material in which the core is made up of strong fibres lying approximately normal to the plane of the sheet (HSSA), adhesively bonded to the faceplates, the value was about 340 J m^{-2} . For the other two types of material, in which the core comprised softer fibres lying close to the plane of the sheet, adhesively bonded or brazed to the faceplates, the value was much lower at about 30 J m^{-2} . There were no significant differences between the values obtained for these two materials.
- (b) The HSSA delaminated by pull-out of fibres from their sockets in the adhesive. A model has been developed simulating the energy absorbed during operation of this mechanism, based on simple shear-lag theory. Good agreement is found between theory and experiment, assuming an interfacial shear strength between fibre and adhesive of about 5 MPa . This is a plausible value, although towards the lower end of typical fibre-matrix shear strengths, and the analysis indicates that improvements in this bond strength, which should be achievable by fibre surface treatments etc., would lead to enhancement of the delamination fracture energy.
- (c) The other two materials both failed by fracture of fibres within the core. Since their core struc-

tures were identical, the observation that their fracture energies were similar is entirely expected. A model has been developed for prediction of the fracture energy for this type of failure. In order to obtain agreement with experiment, it was necessary to postulate a rather narrow zone within the core in which the fibres broke and deformed. This was not really consistent with what was observed. It is suggested that the low value may be partly due to a tendency wherever possible for delamination to occur by failure of sintered fibre–fibre necks, rather than by fibre fracture. A higher fracture energy would be expected if these necks could be strengthened, and also if the fibre strength could be raised. In general, having the fibres lying at low angles to the plane of the sheet does not lead to good fracture toughness values (or to favourable stiffness characteristics—see Part I).

Acknowledgements

Support has been provided for AEM via the Cambridge-MIT Institute (CMI). Acknowl-

edgement is also due to R.N-G. Gustafsson (Volvo Technological Development Corporation, Sweden) and J. Karlsson (HSSA AB, Sweden) for many useful discussions and for providing the HSSA material.

References

- [1] Sorensen BF, Horsewell A, Jorgensen O, Kumar AN. Fracture resistance measurement method for in situ observation of crack mechanisms. *J. Am. Ceram. Soc.* 1998;81:661–9.
- [2] Hull D, Clyne TW. An introduction to composite materials. In: Clarke DR, Suresh S, Ward IM, editors. *Cambridge solid state science series*. Cambridge: Cambridge University Press; 1996.
- [3] DiFrancia C, Ward TC, Claus RO. The single-fibre pull-out test I. Review and interpretation. *Composites A* 1996;27:597–612.
- [4] Kim JK, Baillie C, Mai YW. Interfacial debonding and fibre pull-out stresses. Part I—critical comparison of existing theories with experiments. *J. Mat. Sci.* 1992;27:3143–54.